Research Article

Effects of 15th January 2010 Annular Solar Eclipse on Traveling Ionospheric Disturbances and Equatorial Plasma Bubbles over Low Latitude Regions of East Africa

Davis Odhiambo Athwart [ID],[1] Boniface Ndinya [ID],[1] and Paul Baki [ID][2]

[1]*Department of Physics, Masinde Muliro University of Science & Technology, P.O. Box 190-50100, Kakamega, Kenya*
[2]*Department of Physics & Space Science, Technical University of Kenya, P.O. Box 52428-00200, Nairobi, Kenya*

Correspondence should be addressed to Davis Odhiambo Athwart; athwartdavis@gmail.com

The influence of the 15th January 2010 annular solar eclipse on traveling ionospheric disturbances (TIDs) and equatorial plasma bubbles (EPBs) is studied using data from six global navigation and satellite system (GNSS) receivers spread across the path of annularity over the low latitude region of East Africa. The GNSS receivers are stationed at Nairobi (RCMN), Malindi (MAL2), and Eldoret (MOIU) in Kenya; Mbarara (MBAR) in Uganda; Kigali (NURK) in Rwanda; and Mtwara (MTWA) in Tanzania. The study period ranges from 12th to 18th January 2010, three days before and after the 15th January 2010 annular solar eclipse. The year 2010 marked the beginning phase of solar cycle 24, evidently observed in low total electron content (TEC) values and the disturbed storm time index (Dst). The eclipse started at 7 : 06 LT and ended at 10 : 14 LT, with MOIU and RCMN experiencing eclipse magnitudes of 0.946 and 0.93, respectively. The maximum obscuration occurred between 8 : 21 LT and 8 : 34 LT across most of the stations. A detrending on vertical TEC (VTEC) derived from GNSS receivers across or close to the path of totality revealed a reduction of ~2-3 TECU during the maximum phase of the eclipse. The level of reduction was highly close to the totality path and decreased smoothly away from the totality path. Using a background polynomial fitting technique on diurnal TEC, we analyzed TIDs along NURK-MBAR-MOIU and MOIU-RCMN-MAL2 GPS arrays. The results revealed a wavelike perturbation with a virtual horizontal velocity of 830m/s and ~1 TECU amplitude propagating eastward along the MOIU-RCMN-MAL2 GPS array. The study reports a moderate scintillation activity of $0.5 \leq ROTI \leq 0.9$ values, demonstrating the presence of few EPBs over the region. The results show a latitudinal variation in GPS-TEC scintillation activities and suggest a possible influence of the eclipse on the observed increase in average scintillation levels across East Africa.

1. Introduction

A solar eclipse happens when the Moon moves in front of the Sun and blocks its light entirely or partially on a portion of the Earth's surface, causing the solar illuminance changes for a short time [1], which also offers a rare chance to study the ionospheric reaction to the sudden cessation of solar radiation [2, 3]. The total solar eclipse only lasts for a few minutes in any given location due to the supersonic speed of the Moon's shadow traveling eastward across the Earth. Due to various Sun-Moon-Earth alignment geometries and varied lunar orbital properties, it does not repeat in any

discernible pattern [4]. The ionosphere's response to a solar eclipse is influenced by a number of variables, including the sun's activity, the geomagnetic environment, the location, latitude, and longitude, and the time of day [3].

The rapid fluctuations in solar electromagnetic flux and ionizing ultraviolet (UV) radiation that occur during eclipses have a variety of impacts on the thermosphere and ionosphere, including a change in the temperature balance and the generation and loss of ionization in the lower ionosphere [5]. The eclipse alters the ionization in the E and F regions of the ionosphere where dynamic processes are crucial. As a result, the ionosphere is likely to be

considerably affected both during and after a solar eclipse. Ionospheric response to solar eclipses at low latitudes and the underlying physical mechanisms is still an open question [6]. However, inconclusive results of solar eclipse observations arise from the fact that different solar eclipses produce different plasma motions [7].

Due to recent developments in radio remote sensing technology, the effects of solar eclipses on the ionosphere may now be continuously monitored over a wide area. Studying ionospheric dynamics across East Africa is now possible thanks to the installation of global navigation and satellite systems (GNSS) receivers throughout the region. During a solar eclipse, the total electron content (TEC), produced by the Global Positioning System (GPS) receivers, is a reliable indicator of the condition and dynamics of the ionospheric F-region [8, 9].

Solar eclipses are known to generate atmospheric gravity waves (AGWs) [10, 11]. AGWs induce traveling ionospheric disturbances (TIDs) via neutral-ion collisions [12]. TIDs are evident as fluctuations in TEC derived from GPS receivers [14]. Although these TIDs appear to be self-propagating, they are not. If the underlying AGW dissipates, the TID will disappear because of the lack of neutral-ion collisions. Therefore, TIDs induced by AGWs are not exact tracers of the AGWs. However, their presence does indicate the existence of underlying AGWs, which can be quite useful for diagnosing AGWs and their sources [14]. The source of the AGWs could be located by combining observations from three stations using a reverse ray-tracing technique [3]. A differential total electron content (ΔTEC) approach detects tiny spatially coherent disturbances caused by numerous physical mechanisms [15]. Local conditions such as local time, background wind, and topography might affect AGW propagation, causing significant variation in the ionospheric electron density during an eclipse [16].

A study by Emirant [17] on the ionospheric response to the 3rd November 2013 solar eclipse showed that TEC over East Africa was modified by wave-like energy and momentum transport. When studying detection and description of the different ionospheric disturbances that appeared during the solar eclipse of 21st August 2017 over the United States, Heng [18] observed medium-scale TIDs (MSTIDs) with wavelength and velocity in the range of 250–300 km and 150–300 m/s, respectively, propagating in the same direction as that of the lunar disc during the early stages of the eclipse transit. The MSTIDs were detected less than 30 minutes after the eclipse's onset. Earlier observations during the same eclipse event over North America by Zhang [12] revealed strong solar eclipse-induced ionospheric bow waves with a wavelength ranging between 270 and 350 km, a 25-minute period and a phase velocity of 280 m/s in a direction aligned with totality. In a study to investigate the effects of the 15th January 2010 solar eclipse event on equatorial and low latitude regions of India, Panda [19] observed that the faster downward movement of plasma was the primary cause of increased electron density over the equator and substantially decreased TEC at all latitudes. When investigating the ionospheric response over South America during the 2nd July 2019 total solar eclipse using the Chilean GPS eyeball, [16] observed AGWs with a period of 30 to 60 minutes at the station located north of totality.

The intensity of ionospheric scintillations is frequently described quantitatively using the rate of change of TEC index (ROTI) [20, 21]. Equatorial plasma bubbles (EPBs) are believed to be the dominant source of irregularities that cause scintillation of the GPS satellite signals at L band frequencies [22, 23]. Values of ROTI ≥ 0.5 TECU/min are considered moderate scintillation activities [24], which could potentially reveal the presence of EPBs. Strong scintillation in the signal amplitude and phase contributes to the loss of lock on GPS signals, decreasing the number of available satellites and consequently reducing the possibility to get good satellite geometry, hence degrading navigation and positioning measurements [25]. A study by Norsuzila [26] on the effect of the 15th January 2010 solar eclipse over Malaysia also reported a reduction in TEC and amplitude scintillation. When examining the effects of the 21st August 2017 total solar eclipse on variations of TEC over the North American region, the author found that the solar eclipse decreased ionospheric scintillation occurrence at the totality region by up to 28 percent and TEC values decreased by up to 7 TECU [27].

We report the effects of the 15th January 2010 annular solar eclipse on low-latitude TIDs and EPBs over the East Africa region using data from GNSS receivers stationed at Nairobi (RCMN), Malindi (MAL2), and Eldoret (MOIU) in Kenya; Mbarara (MBAR) in Uganda; Kigali (NURK) in Rwanda; and Mtwara (MTWA) in Tanzania.

2. Materials and Methods

2.1. Preparation and Processing of Data. The 15th January 2010 annular solar eclipse was visible across most parts of the East Africa region, with RCMN and MOIU receiver stations being along the umbra path, while MAL2, NURK, MBAR, and MTWA receiver stations were along the penumbral path of the eclipse. Generally, the eclipse onset was at 07 : 06 LT, reaching its maximum phase at about 08 : 28 LT and ending at 10 : 14 LT. The period of annularity lasted between 6 and 8 minutes. Further details are available at https://eclipse.gsfc.nasa.gov/SEmono/ASE2010/ASE2010.html. The geographic locations of the six GNSS receivers, namely, RCMN, MOIU, MAL2, NURK, MBAR, and MTWA are given in Figure 1.

Table 1 shows the geographic latitude (GLAT), geographic longitude (GLON), geomagnetic latitude (MLAT), and geomagnetic longitude (MLON) of the GNSS receiver stations, obtained from http://wdc.kugi.kyoto-u.ac.jp/igrf/gggm/index.html.

The data used for this research for the period between 12th and 18th January 2010 were obtained from the GNSS receivers stations at six locations over the East African region, as shown in Figure 1. The data for each GNSS receiver stations were downloaded from https://cddis.gsfc.nasa.gov/pub/gps/data/daily/ in receiver independent exchange (RINEX) format. The TEC values for each station were derived using the GPS-TEC algorithm developed by [28]. The application first calculates the relative values of slant TEC (STEC) by eliminating the effect of tropospheric water
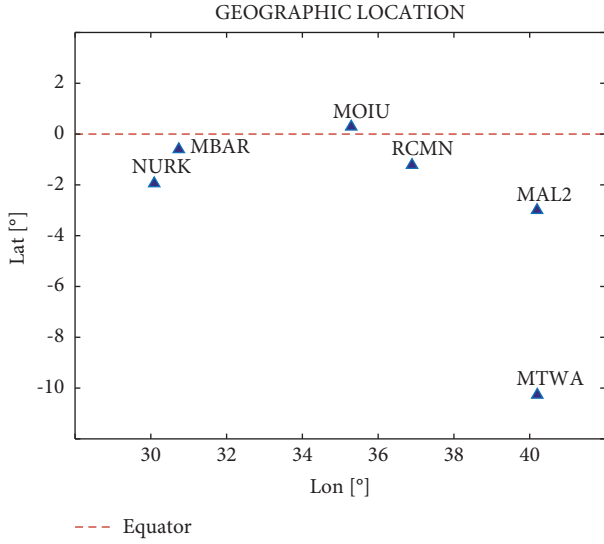
FIGURE 1: Geographic location of the GNSS receiver stations over East Africa.

vapor and clock errors using the phase and code values of the two GPS frequencies [29], then later the absolute value after compensating for the satellite and receiver biases. The absolute STEC along the oblique signal paths are also mapped to vertical TEC (VTEC) values at the ionospheric pierce point (IPP) assumed to be 350 km by means of the single layer model (SLM) mapping function [30, 31]. The VTEC values were sampled at 30-second intervals.

2.2. Traveling Ionospheric Disturbances (TIDs). To determine the background or unperturbed ionospheric TEC, each satellite's time series of vertical TEC data were fitted with a fourth-order polynomial across all stations. The equation for the fourth-order polynomial fitting is

$$VT^f (t)_{ij} = at_{ij}^4 + bt_{ij}^3 + ct_{ij}^2 + dt_{ij} + \varepsilon, \tag{1}$$

where $VT^f (t)_{i,j}$ is fitted TEC at time t, $i = 1, 2, \ldots, 6$ (no. of receiver stations), $j = 1, 2, \ldots, 31$ (no. of satellites), coefficients a, b, c, and d are obtained through the least squares method, and ε is the residual error of the fitting process [32]. The dominant periods of the structures observed, were obtained using detrended TEC (ΔTEC), expressed as

$$\Delta TEC (t)_{i,j} = TEC_{i,j} - VT^f (t)_{i,j}, \quad \forall i, j, \tag{2}$$

where $TEC_{i,j}$ is the actual TEC at time, t, and $\forall i$, j implies for all i and j receiver stations and satellites, respectively. By monitoring $\Delta TEC (t)_{i,j}$, the amplitude of the wavelike structures (TIDs) that modulate TEC were inferred [32, 33].

The virtual horizontal velocities of the TIDs were calculated by monitoring the time delays between consecutive peaks and troughs of the wavelike structures and determining the horizontal distances between the GNSS receiver stations [34]. The potential wavelike structures were monitored across three stations along similar or close latitudes. The horizontal distances between stations along the NURK-MBAR-MOIU and MOIU-RCMN-MAL2 arrays, as shown in Table 2, were calculated using the following equation:

$$\Delta d = R_E \Delta \sigma, \tag{3}$$

where R_E is the radius of the Earth and $\Delta \sigma$ is the central angle between two receivers given as

$$\Delta \sigma = \arctan \left(\frac{\sqrt{\left[\cos \theta_f \sin (\Delta \varnothing)^2 \right] + \left[\cos \theta_s \sin \theta_f - \sin \theta_s \cos \theta_f \cos (\Delta \varnothing) \right]^2}}{\sin \theta_s \sin \theta_f + \cos \theta_s \cos \theta_f \cos (\Delta \varnothing)} \right), \tag{4}$$

where $\Delta \varnothing = |\varnothing_s - \varnothing_f|$, with the subscript s for the first latitude/longitude and subscript f for the second latitude/longitude [35].

2.3. Equatorial Plasma Bubbles (EPBs). The rate of change of TEC (ROT) was calculated for every considered GNSS station and then detrended for all individual satellite tracks using the equation:

$$ROT = \frac{TEC_k^i - TEC_{k-1}^i}{\Delta t}, \tag{5}$$

where i is the visible satellite, k is the time of epoch, $k-1$ is the subsequent time of epoch, and Δt is the time difference (60 seconds). ROTI, defined as the standard deviation of the detrended ROT values [36], was calculated using the following equation:

$$ROTI = \sqrt{\langle ROT^2 \rangle - \langle ROT^2 \rangle}. \tag{6}$$

The presence of EPBs is inferred by monitoring the intensity of ionospheric scintillations. A value of ROTI ≥ 0.5 TECU/min is considered moderate scintillation activity [24] and could potentially reveal the presence of EPBs.

3. Results and Discussion

3.1. Effect of the Eclipse on TEC. Figure 2 shows the daily mean VTEC over all stations for days 12th to 18th January 2010, with a minimum of 14.19 TECU and a maximum of 19.78 TECU. Only NURK (Figure 2(f)) shows considerable decline in daily mean VTEC values on the eclipse day (15th day) in comparison with the 14th and 16th day. Generally, the eclipse impact on daily mean TEC variation was not so pronounced since the year 2010 marked the beginning phase of the solar minimum of solar cycle 24.

TABLE 1: Geophysical parameters of the dual frequency GNSS receiver stations.

Country	Station	Code	GLAT (°)	GLON (°)	MLAT (°)	MLON (°)
Kenya	Malindi	MAL2	2.9960°S	40.194°E	6.73°S	111.62°E
Kenya	Eldoret	MOIU	0.2883°N	35.290°E	2.70°S	107.30°E
Kenya	Nairobi	RCMN	1.2210°S	36.894°E	4.45°S	108.63°E
Rwanda	Kigali	NURK	1.9446°S	30.090°E	4.02°S	101.79°E
Uganda	Mbarara	MBAR	0.6015°S	30.738°E	2.82°S	102.66°E
Tanzania	Mtwara	MTWA	10.268°S	40.200°E	13.86°S	110.42°E

TABLE 2: Distances between stations along similar or close latitudes.

Stations	Distance (km)
MOIU (Eldoret, Kenya)—RCMN (Nairobi, Kenya)	244.3814
RCMN (Nairobi, Kenya)—MAL2 (Malindi, Kenya)	416.2906
MBAR (Mbarara, Uganda)—MOIU (Eldoret, Kenya)	516.2000
NURK (Kigali, Rwanda)—MBAR (Mbarara, Uganda)	165.0979

To monitor TEC variations, we obtained the detrended TEC over MOIU, RCM, MAL2, MBAR, NURK, and MTWA receiver stations on 15th January 2010, during the onset, maximum, and offset phases of the eclipse as shown in Figure 3.

In Figure 3, RCMN, MAL2, MBAR, and MOIU stations that were either within or close to the path of totality during the maximum phase of the eclipse showed a considerable decline in TEC of 1-2 TEC units. The moon occulted the sun's radiation over the East African region, thus briefly preventing photoionization. This was evident, especially during the maximum phase of the eclipse at about 08 : 27 LT. Similar results were observed by [37] when studying the effect of the 15th January 2010 solar eclipse over the Indian region, in which a decline in TEC during the eclipse period was dependent on the station's proximity to the eclipse path.

3.2. Effect of the Eclipse on TIDs.

TIDs normally manifest themselves as plasma density fluctuations which propagate as a wave away from the region of totality. Since TIDs are known to modulate TEC, we investigated TEC enhancements and depletions observed across receiver stations along similar or close latitudes. The GNSS receiver station arrays investigated were NURK-MBAR-MOIU and MOIU-RCMN-MAL2, thus giving longitudinal variation regarding the TIDs propagation. Figure 4 shows the graph of VTEC and fitted VTEC against local time (LT) across NURK-MBAR-MOIU and MOIU-RCMN-MAL2 station arrays on 15th January 2010.

In Figure 4, the TEC perturbations manifesting as a wave-like structure along the arrays are presented as a double peak, indicated by the arrows before and during the eclipse period. The first peak is observed between 4 : 00 LT and 5 : 00 LT, while the second peak is observed between 7 : 00 LT and 8 : 30 LT. Although the first peak is not quite visible along the NURK-MBAR-MOIU array, it is significantly noticeable along the MOIU-RCMN-MAL2 array. For the MOIU-RCMN-MAL2 GPS array, the first peak is observed at MOIU, then RCMN, and finally MAL2 station, with the time of contact being about 06 : 50 LT, 07 : 05 LT,

and 07 : 10 LT, respectively. The virtual horizontal velocity of the observed wave-like perturbation was calculated using time delays between the peaks of structures observed and the horizontal distances presented in Table 2. The average virtual horizontal velocity of the wave-like perturbation was found to be 830 m/s in the eastward direction. Since the wavelike structure is observed at the same time as the eclipse and propagates in the same direction as the lunar disc, it could potentially be influenced by the eclipse event. The detrended TEC plots revealing the amplitude of the perturbation along NURK-MBAR-MOIU and MOIU-RCMN-MAL2 receiver array on 15th January 2010 are shown in Figure 5.

In Figure 5, a TEC depletion of about 1.5 TECU was observed along NURK-MBAR-MOIU and MOIU-RCMN-MAL2 receiver array on 15th January 2010, the eclipse day. This is because these stations were either along or close to the path of totality of the eclipse.

Figures 6–11 show plots of actual and fitted VTEC against local time (LT) across NURK-MBAR-MOIU and MOIU-RCMN-MAL2 station arrays on 12th, 13th, 14th, 16th, 17th, and 18th January 2010, respectively.

We note in Figures 6–11 that the control days, 12th, 13th, 14th, 16th, 17th, and 18th January 2010, respectively, did not reveal similar wave-like structures. The VTEC perturbations observed across different arrays in Figures 6–11 did not reveal continuous propagation of any wavelike structures. Thus, there was minimal perturbation from the background VTEC on the control days, 12th, 13th, 14th, 16th, 17th, and 18th January 2010 resulting from an underlying propagating disturbance at ionospheric heights.

3.3. Effects of the Solar Eclipse on Ionospheric Scintillations.

The ROTI derived from TEC observations is a good proxy for ionospheric scintillations. The plots of ROTI against LT derived from equation (6) are presented in Figures 12–17 for RCMN, MAL2, MOIU, MBAR, MTWA, and NURK stations, respectively.

In Figure 12, the highest ROTI value of 0.9 TECU/min between 20 : 00 LT and 23 : 00 LT was observed over the RCMN station on 15th January 2010. Clearly, there was more intense ionospheric scintillation over RCMN station on the
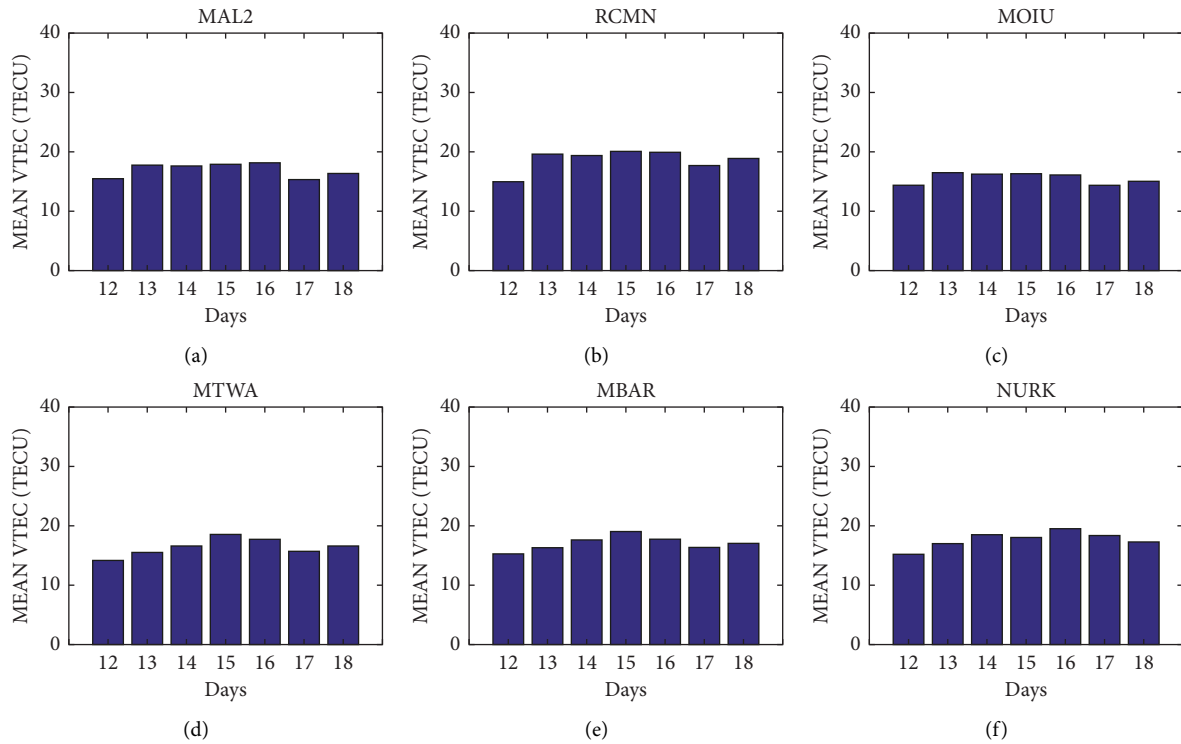
FIGURE 2: Daily mean VTEC over (a) MAL2, (b) RCMN, (c) MOIU, (d) MTWA, (e) MBAR, and (f) NURK stations for days 12th to 18th January 2010.
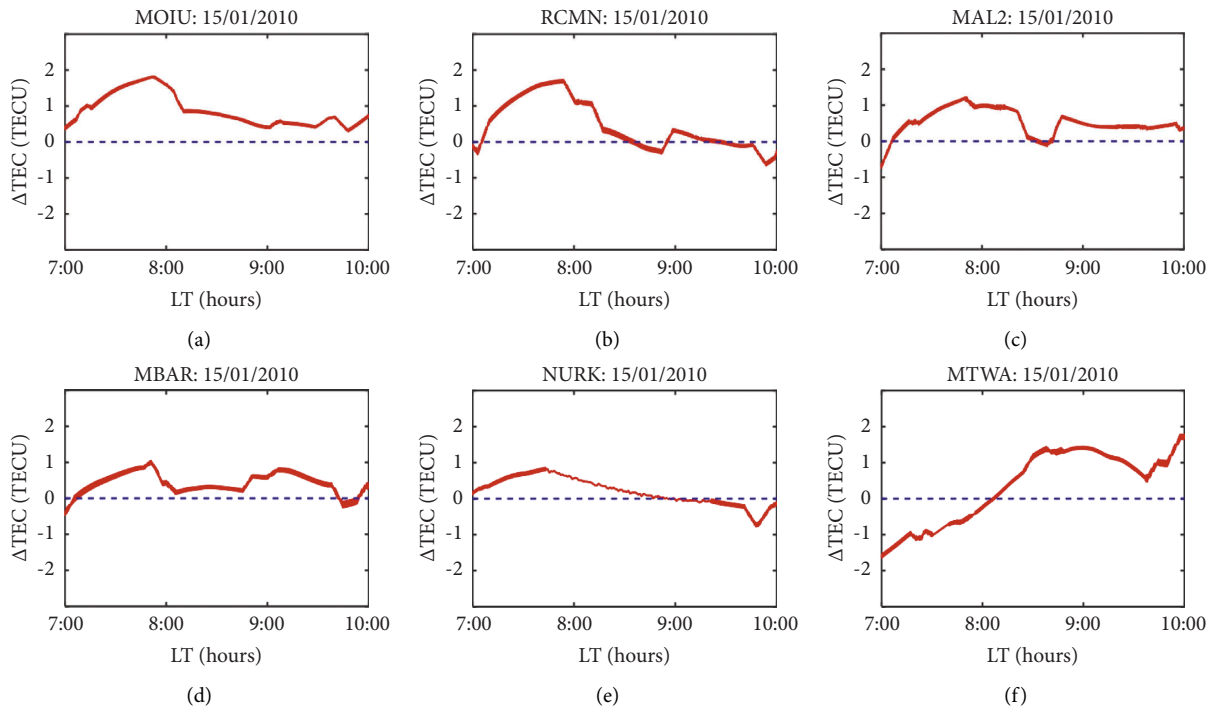

FIGURE 3: The detrended TEC (red line) and mean level (blue line) variation with local time (LT) over (a) MOIU, (b) RCM, (c) MAL2, (d) MBAR, (e) NURK, and (f) MTWA on 15th January 2010.
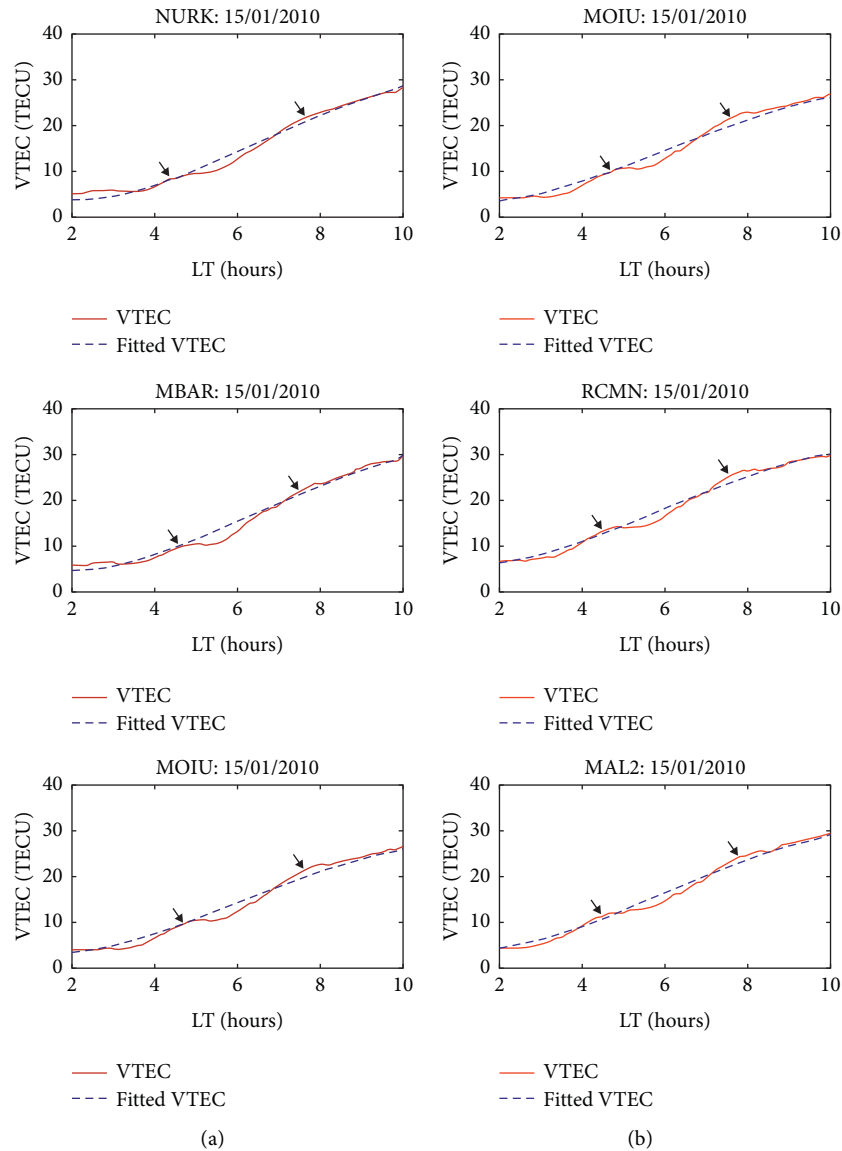
FIGURE 4: VTEC and fitted VTEC against local time (LT) across (a) NURK-MBAR-MOIU and (b) MOIU-RCMN-MAL2 GPS array on 15th January 2010.

eclipsed day than on the control days. It is important to note that the RCMN station was within the path of totality.

In Figure 13, the MOIU receiver station experienced weak scintillation activities both on the eclipsed day and control days as observed even though it was along the path of totality.

In Figure 14, the MAL2 station experienced two moderate ionospheric scintillation events on 12th and 15th January 2010 with ROTI values of 0.45 TECU/min and 0.5 TECU/min, respectively, occurring between 20 : 00 and 23 : 00 LT.

In Figure 15, the MBAR station had the highest ROTI value of 0.4 TECU/min, occurring between 20 : 00 and 23 : 00 LT on 12th January 2010. The eclipsed day, however, did not reveal significant scintillation activities.

Figure 16 shows that most of the days over MTWA station, including the eclipsed day, had an average ROTI value of 0.1 TECU/min. Therefore, the ionosphere over MTWA station had no major plasma density depletions that could potentially cause strong GPS signal scintillation. There was no observed eclipse effect on EPBs over MTWA. This could be due to its proximity to the path of annularity as compared with other stations.

In Figure 17, NURK station had the highest ROTI value of about 0.5 TECU/min between 20 : 00 and 22 : 00 LT on 12th January 2010. The eclipsed day, however, did not reveal significant scintillation activities.

Generally, as shown in Figures 12–17 for RCMN, MAL2, MOIU, MBAR, MTWA, and NURK stations, respectively, there were minimal scintillation events with
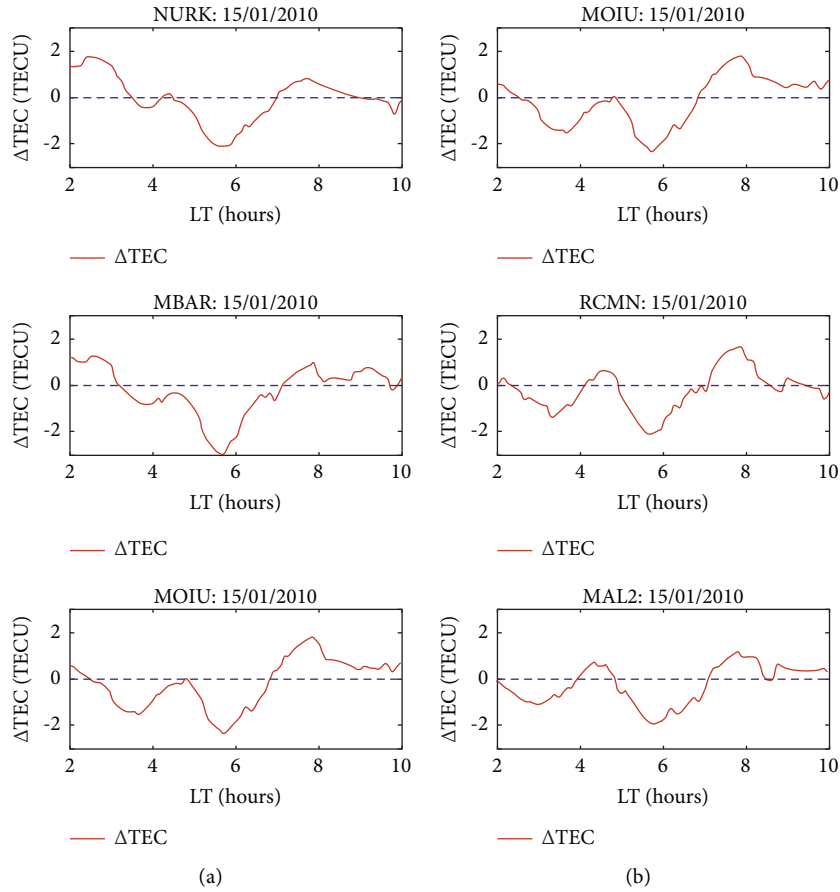
FIGURE 5: The detrended TEC (red line) and mean level (blue line) variation with local time (LT) across (a) NURK-MBAR-MOIU and (b) MOIU-RCMN-MAL2 receivers array on 15th January 2010.

moderate ROTI values ranging from 0.5 to 0.9 TECU/min observed across all the stations during the period of study. This is in agreement with [38, 39] who reported fewer and moderate GPS scintillations over the same region in January 2010. This implies that there were few plasma density depletions over the East Africa region. Stations closer to the geographic equator, such as RCMN, MBAR, MAL2, and NURK, recorded considerable scintillation events in contrast to MTWA station, which had none. On the eclipse day, 15th January 2010, considerable scintillation events were only observed over RCMN and MAL2 stations, with ROTI values of about 0.9 TECU/min and 0.5 TECU/min, as seen in Figures 12 and 13, respectively. This is because low latitude ionospheric scintillation is known to be a postsunset phenomenon. The influence of the eclipse on TEC earlier in the day was more pronounced over these two stations. However, [27] reported a reduction in scintillation occurrence of up to 28% during the 21st August 2017 solar eclipse over the North American region.
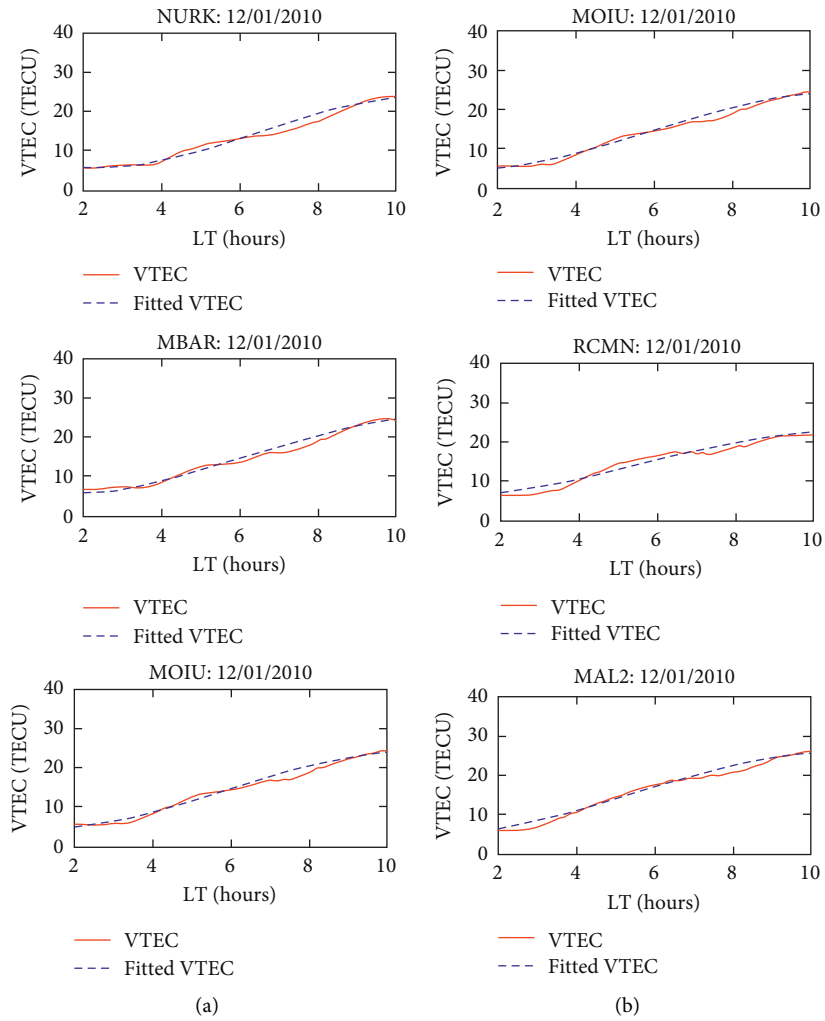
FIGURE 6: VTEC and fitted VTEC against local time (LT) across (a) NURK-MBAR-MOIU and (b) MOIU-RCMN-MAL2 GPS array on 12th January 2010.
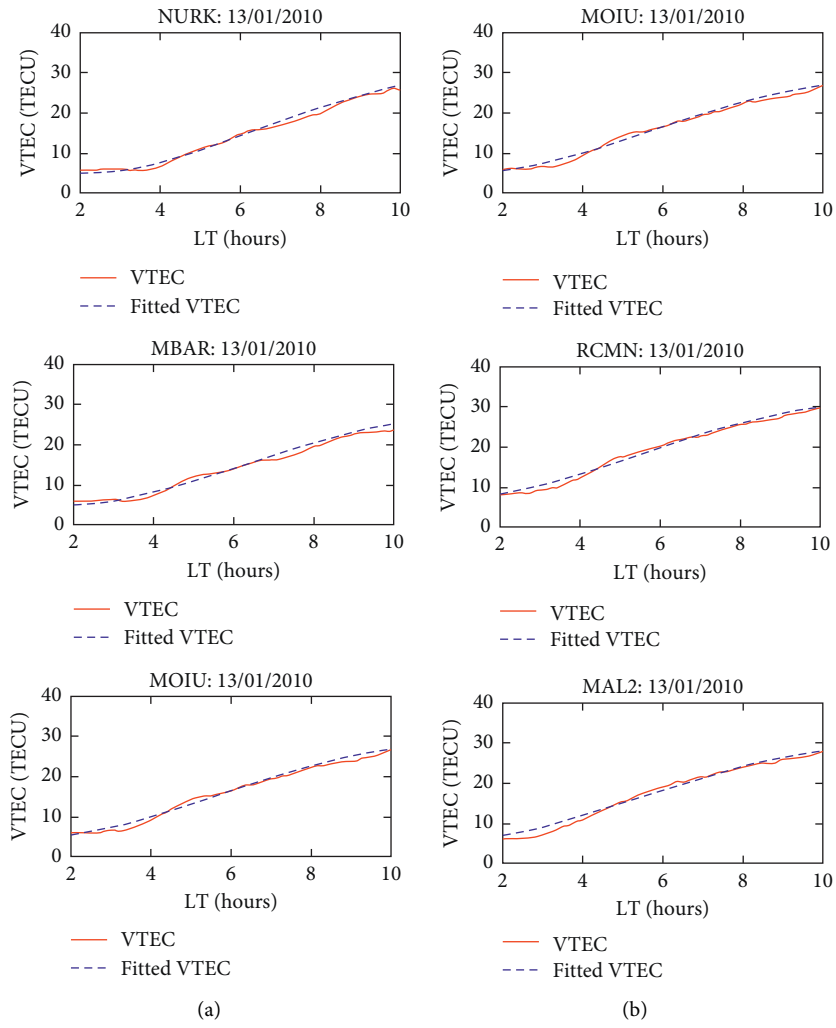
FIGURE 7: VTEC and fitted VTEC against local time (LT) across (a) NURK-MBAR-MOIU and (b) MOIU-RCMN-MAL2 GPS array on 13th January 2010.
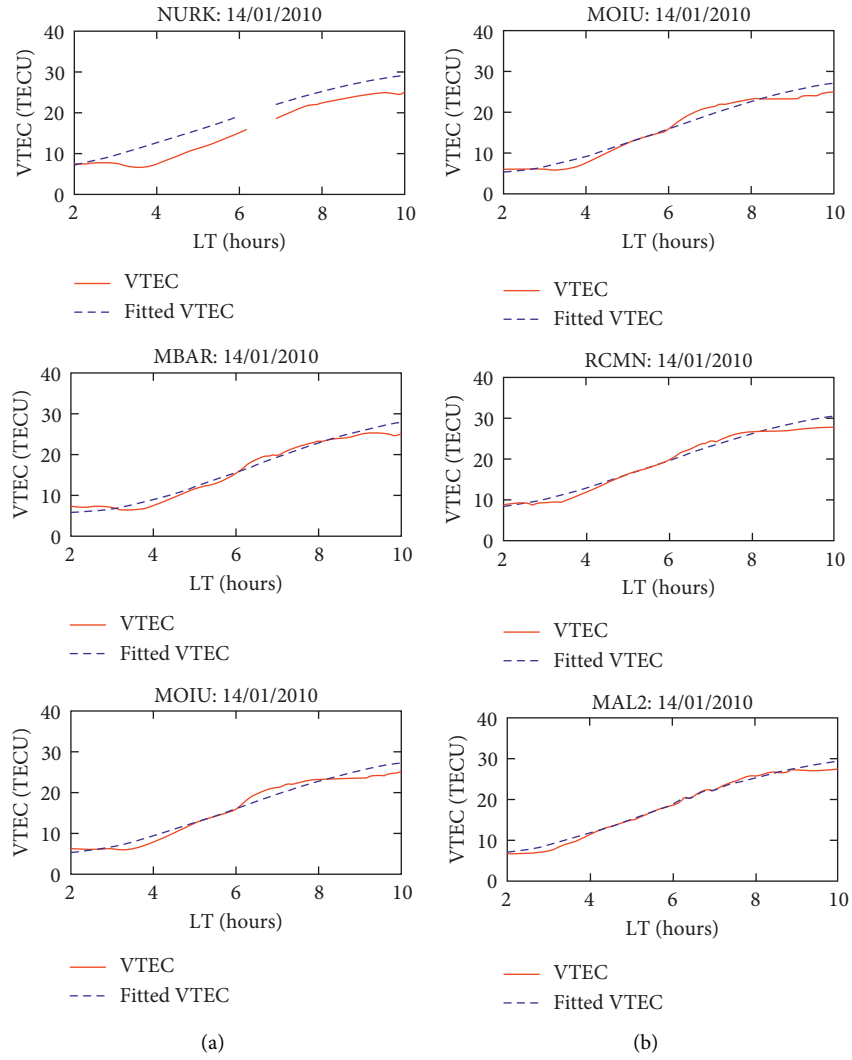
FIGURE 8: VTEC and fitted VTEC against local time (LT) across (a) NURK-MBAR-MOIU and (b) MOIU-RCMN-MAL2 GPS array on 14th January 2010.
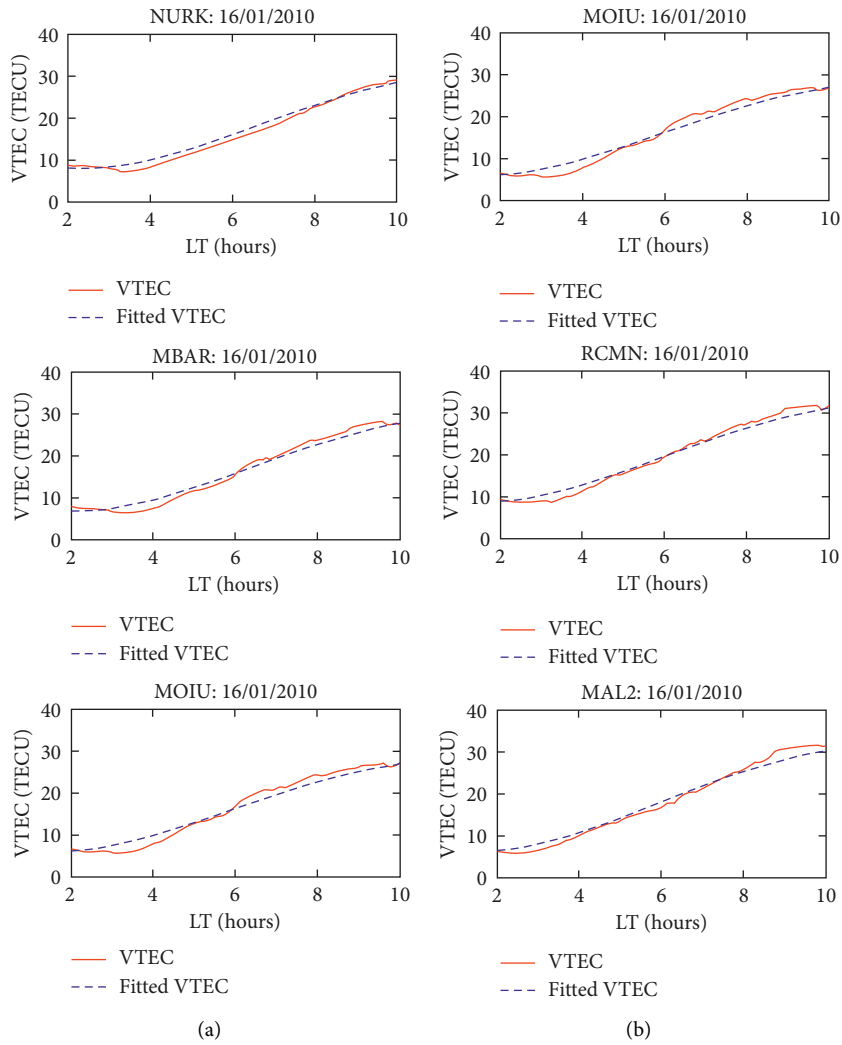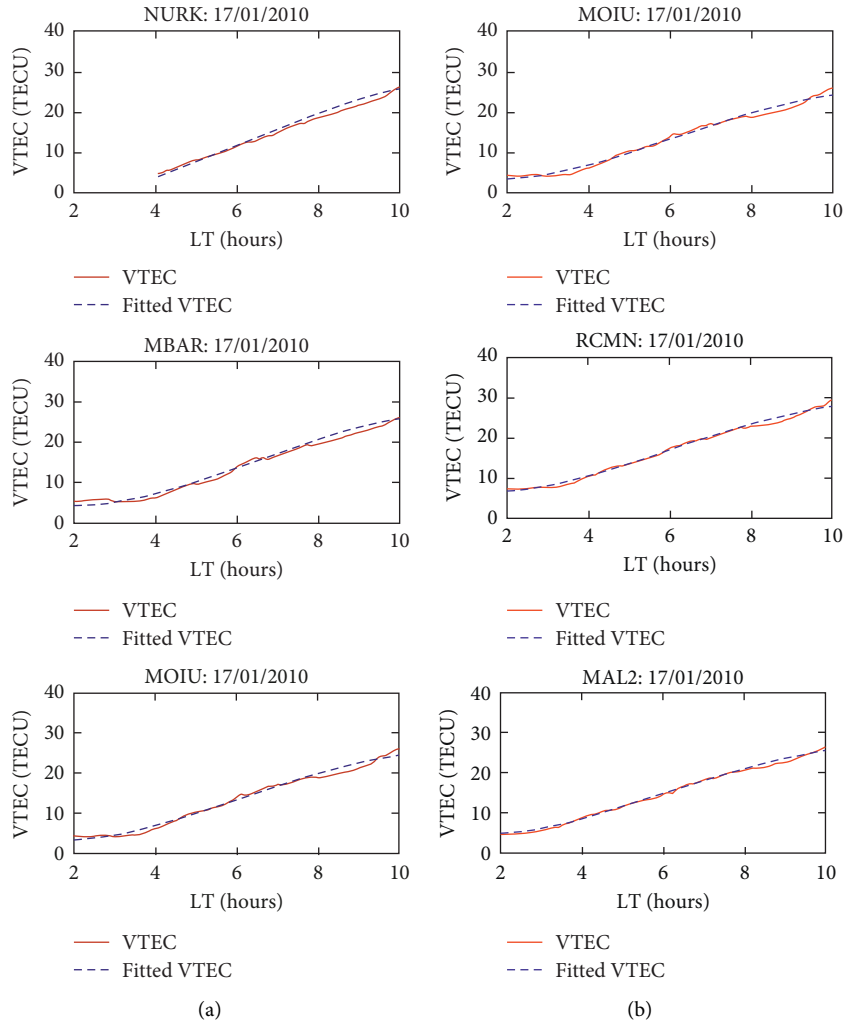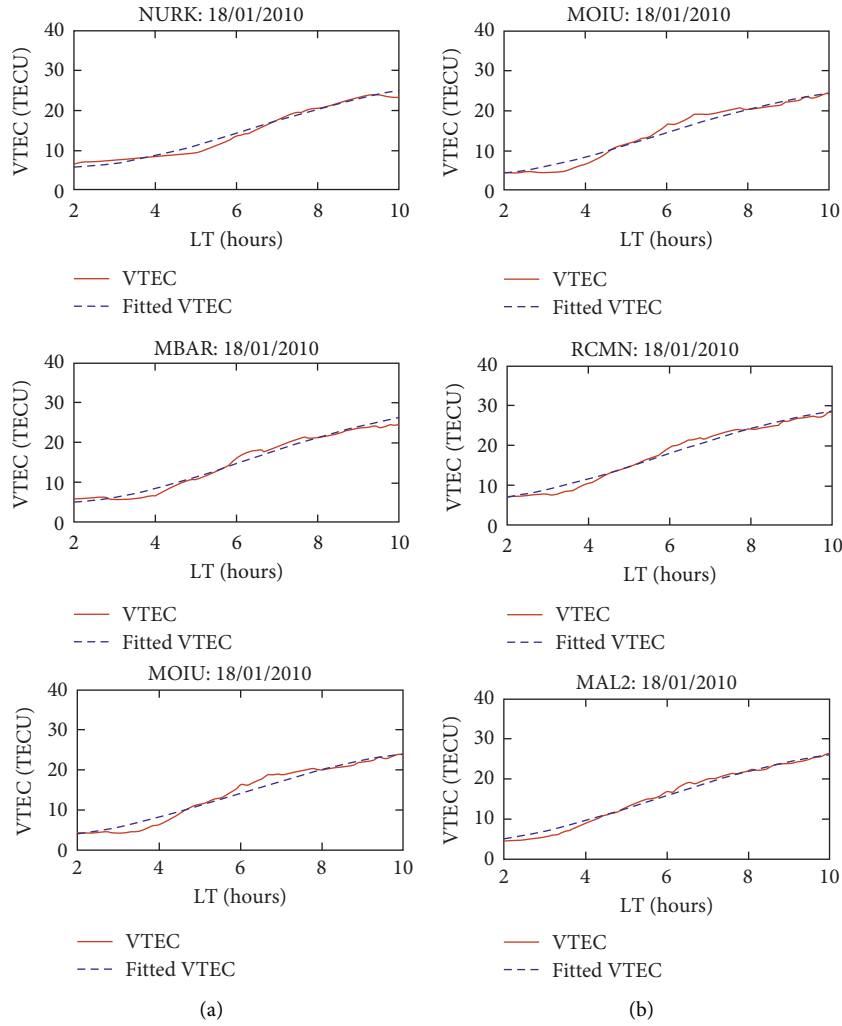
FIGURE 9: VTEC and fitted VTEC against local time (LT) across (a) NURK-MBAR-MOIU and (b) MOIU-RCMN-MAL2 GPS array on 16th January 2010.

Figure 10: VTEC and fitted VTEC against local time (LT) across (a) NURK-MBAR-MOIU and (b) MOIU-RCMN-MAL2 GPS array on 17th January 2010.

FIGURE 11: VTEC and fitted VTEC against local time (LT) across (a) NURK-MBAR-MOIU and (b) MOIU-RCMN-MAL2 GPS array on 18th January 2010.
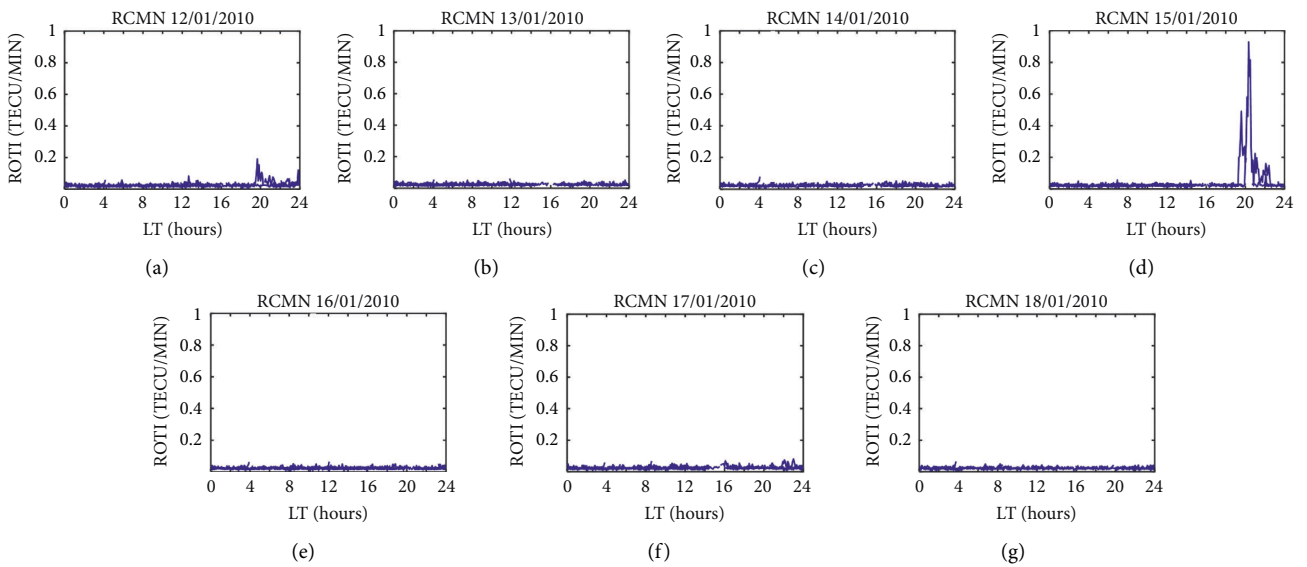

FIGURE 12: ROTI against LT over RCMN station for (a) 12th January 2010, (b) 13th January 2010, (c) 14th January 2010, (d) 15th January 2010, (e) 16th January 2010, (f) 17th January 2010, and (g) 18th January 2010.
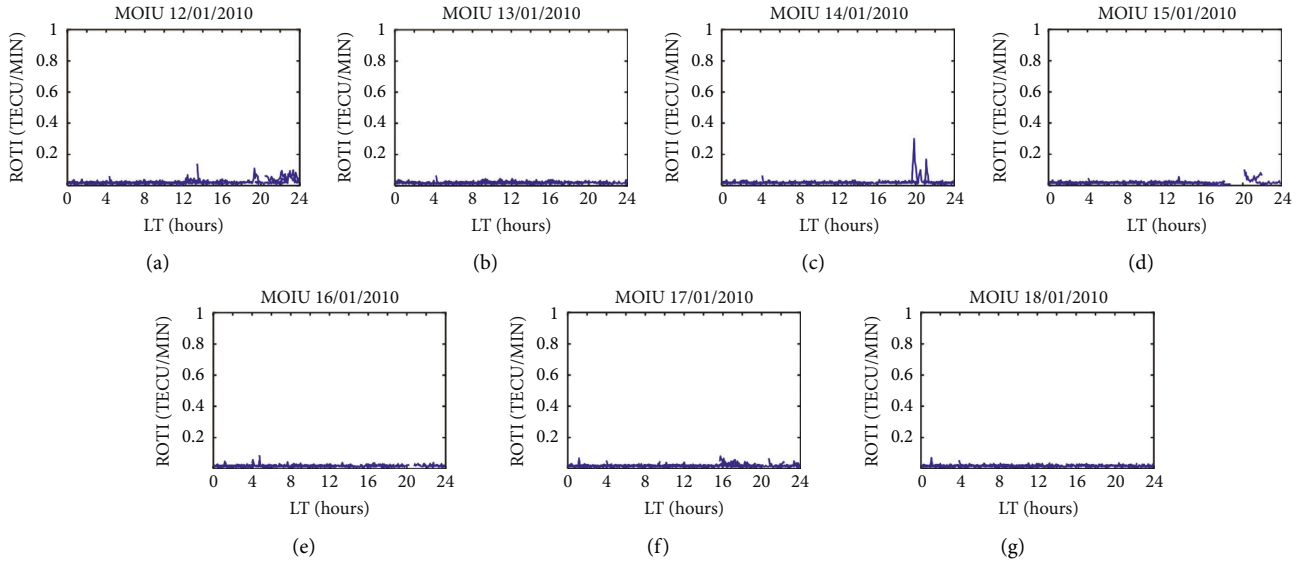
FIGURE 13: ROTI against LT over MOIU station for (a) 12th January 2010, (b) 13th January 2010, (c) 14th January 2010, (d) 15th January 2010, (e) 16th January 2010, (f) 17th January 2010, and (g) 18th January 2010.
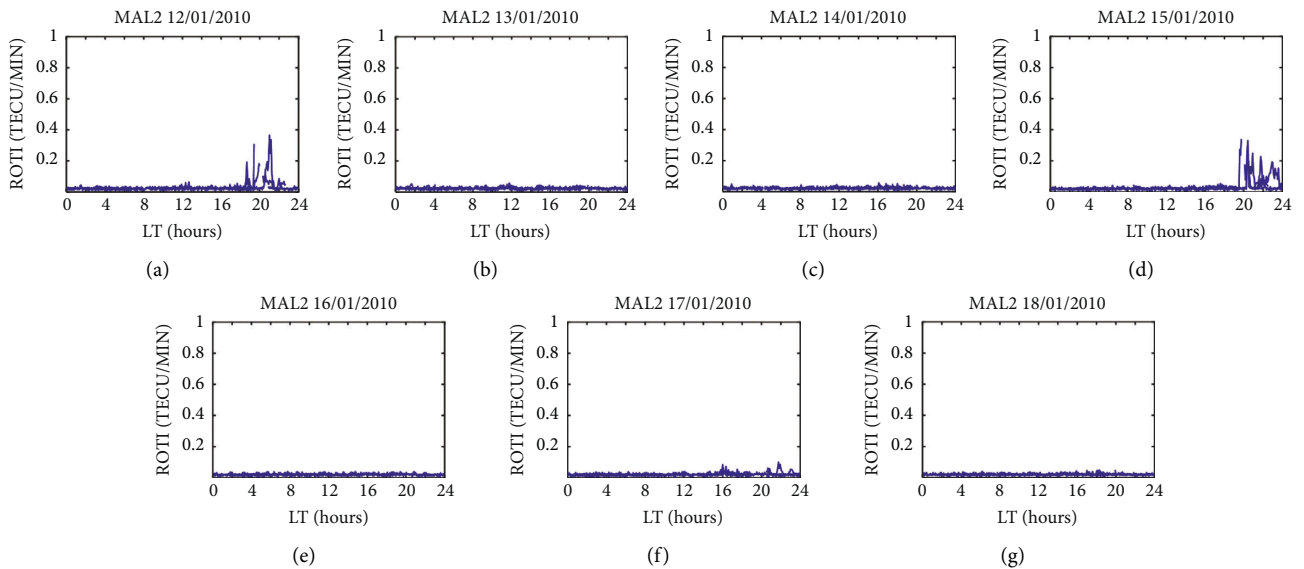

FIGURE 14: ROTI against LT over MAL2 station for (a) 12th January 2010, (b) 13th January 2010, (c) 14th January 2010, (d) 15th January 2010, (e) 16th January 2010, (f) 17th January 2010, and (g) 18th January 2010.
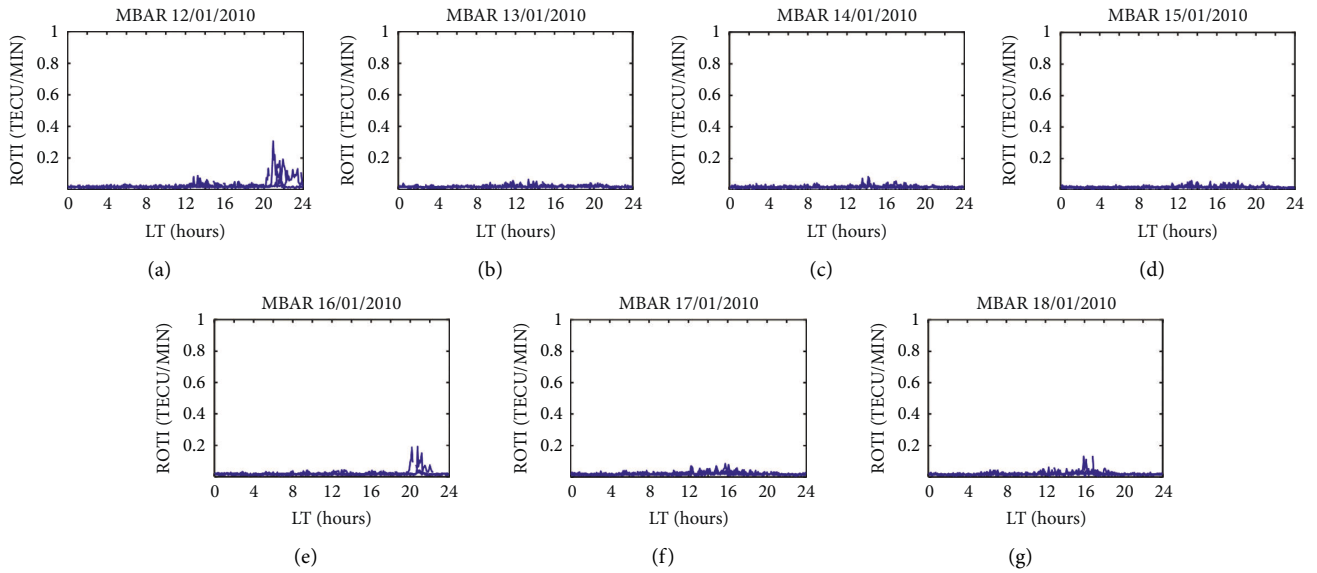
FIGURE 15: ROTI against LT over MBAR station for (a) 12th January 2010, (b) 13th January 2010, (c) 14th January 2010, (d) 15th January 2010, (e) 16th January 2010, (f) 17th January 2010, and (g) 18th January 2010.
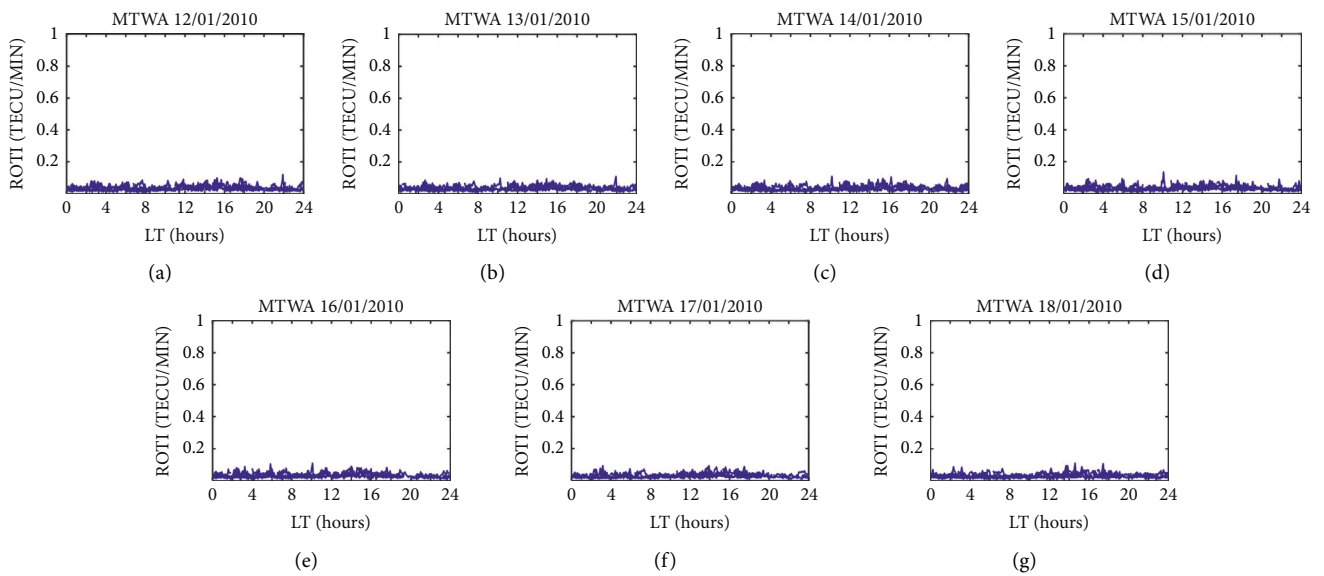
FIGURE 16: ROTI against LT over MTWA station for (a) 12th January 2010, (b) 13th January 2010, (c) 14[th]January 2010, (d) 15th January 2010, (e) 16th January 2010, (f) 17th January 2010, and (g) 18th January 2010.

Figure 17: ROTI against LT over NURK station for (a) 12th January 2010, (b) 13th January 2010, (c) 14th January 2010, (d) 15th January 2010, (e) 16th January 2010, (f) 17th January 2010, and (g) 18th January 2010.
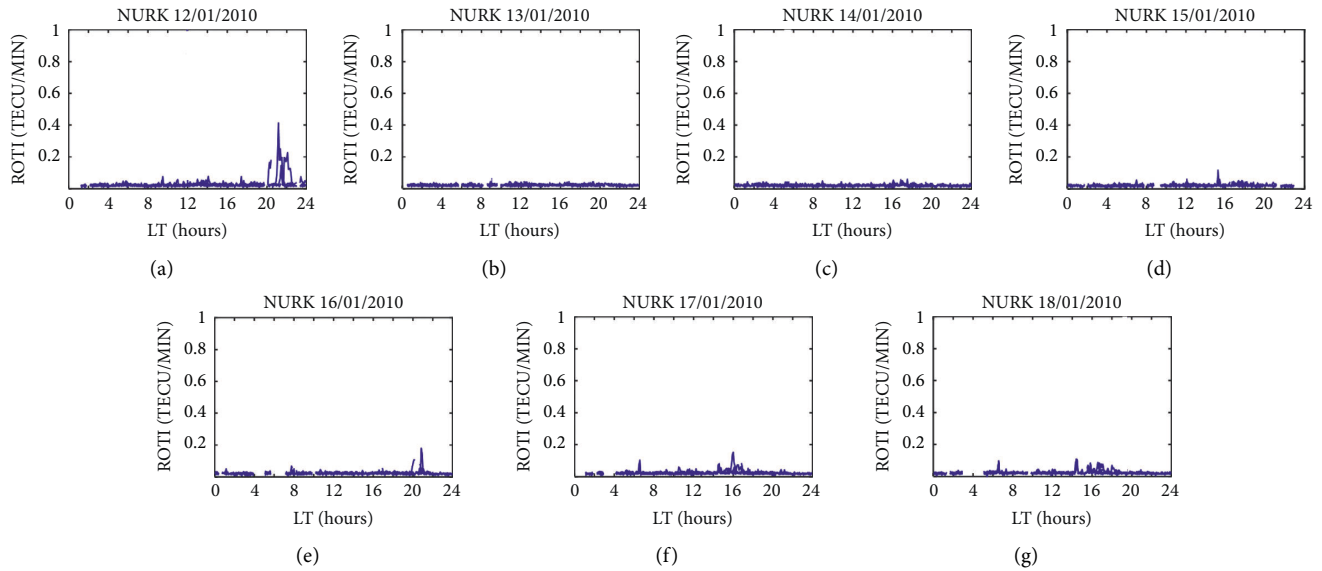
4. Conclusion and Summary

This study presents the first observation of the 15th January 2010 solar eclipse effect on TIDs and EPBs over six stations across the low-latitude regions of East Africa during the ascending phase of the solar minimum of solar cycle 24. The control days were three days before and after the eclipse. TEC depletion was 1.5 TECU along MBAR, MOIU, RCMN, and MAL2 stations. These four stations were either along or close to the totality path of the eclipse. Further analysis revealed the passage of an eastward propagating TID with an average virtual horizontal velocity of 830 m/s along the MOIU-RCMN-MAL2 GPS array during the eclipse period. No TIDs were observed on control days along both GPS arrays. Equatorial plasma bubbles are evident as signal scintillation with values of ROTI ≥0.5. RCMN and MAL2 stations recorded moderate postsunset scintillation levels on the eclipsed day with ROTI values of 0.9 TECU/min and 0.5 TECU/min, respectively, suggesting a possible influence of the eclipse on the occurrence of EPBs, especially over RCMN and MAL2 stations. However, it is not clear why MOIU station being along the totality path showed contrasting observations. Nonetheless, the study reveals evidence of solar eclipse-induced TID propagating eastward in the direction of totality and an increase in scintillation levels over MAL2 and RCMN stations on 15thJanuary 2010. More observations and simulations are necessary to further understand the complex dynamic processes in both the ionospheric and space environment during and after the solar eclipse.

Data Availability

The data that are archived in receiver independent format were downloaded from https://cddis.gsfc.nasa.gov/pub/gps/data/daily/ and used to derive TEC necessary for further analysis.

Conflicts of Interest

The authors declare that there are no conflicts of interest.

Acknowledgments

References

[1] Y. Liu, D. Shen, F. Zhang, and P. Liu, "Using a new sky brightness monitor to observe the annular solar eclipse on 15th january 2010," 2012, https://arxiv.org/abs/1204.4289.

[2] L. Guo, W. M. Zheng, T. Kondo, R. Ichikawa, S. Hasegawa et al., "Ionospheric response to the total solar eclipse of 22 july 2009 as deduced from VLBI and GPS Data," *IVS 2010 General Meeting Proceedings*, pp. 335–339, 2010, http://ivscc.gsfc.nasa.gov/publications/gm2010/li-guo.pdf.

[3] A. Paul, T. Das, S. Ray, A. Das, D. Bhowmick, and A. DasGupta, "Responsed of the equatorial ionosphere to the total solar eclipse of 22 july 2009 and annular eclipse of 15 january 2010 as observed from a network of stations situated in the indian longitude sector," *Annales Geophysicae*, vol. 29, 2011.

[4] F. Espenak and J. Meeus, "Five year millennium canon of solar eclipses," *NASA Technical Paper*, 2006.

[5] H. Rishbeth, "Solar eclipses and ionospheric theory," *Space Science Reviews*, vol. 8, no. 4, pp. 543–554, 1968.

[6] F. Huang, Q. Li, X. Shen et al., "Ionospheric responses at low latitudes to the annular solar eclipse on 21 June 2020," *Journal of Geophysical Research*, vol. 125, 2020.

[7] N. Mahesh, K. Ajeet, and N. Kondapalli, "Ionospheric perturbation during the South American total solar eclipse on 14th december 2020 revealed with the chilean GPS eyeball," *Scientific Reports*, vol. 11, 2021.

[8] H. F. Tsai and J. Y. Liu, "Ionospheric total electron content response to solar eclipses," *Journal of Geophysical Research: Space Physics*, vol. 104, no. A6, pp. 12657–12668, 1999.

[9] B. Vyas and S. Sunda, "The solar eclipse and its associated ionospheric TEC variations over Indian stations on January 15, 2010," *Advances in Space Research*, vol. 49, no. 3, pp. 546–555, 2012.

[10] K. V. Kumar, A. K. Maurya, S. Kumar, and R. Singh, "22 July 2009 total solar eclipse induced gravity waves in ionosphere as inferred from GPS observations over EIA," *Advances in Space Research*, vol. 58, no. 9, pp. 1755–1762, 2016.

[11] C. Nayak and E. Yigit, "GPS-TEC observation of gravity waves generated in the ionosphere during 21 August 2017 total solar eclipse," *Journal of Geophysical Research, Space Physics*, vol. 123, no. 1, pp. 725–738, 2018.

[12] S. Zhang, P. J. Erickson, L. P. Goncharenko, A. J. Coster, W. Rideout, and J. Vierinen, "Ionospheric bow waves and perturbations induced by the 21 August 2017 solar eclipse," *Geophysical Research Letters*, vol. 44, no. 24, 2017.

[13] C. E. Valladares and M. A. Hei, "Measurement of the characteristics of TIDs using small and regional networks of GPS receivers during the campaign of 17–30 July of 2008," *International Journal of Geophysics*, Article ID 548784, 14 pages, 2012.

[14] V. Sharon and A. Irfan, "Concentric secondary gravity waves in the thermosphere and ionosphere over the continetal United States on march 25-26, 2015 from deep convection," *Journal of Geophysical Research Space Physics*, vol. 126, no. 2, 2021.

[15] S. Mrak, J. Semeter, Y. Nishimura, M. Hirsch, and N. Sivadas, "Coincidental TID production by tropospheric weather during the August 2017 total solar eclipse," *Geophyscial Reserch Letters*, vol. 45, no. 20, pp. 10903–10911, 2018.

[16] A. Maurya, M. Shrivastava, and K. Kumar, "ionospheric monitoring with the chilean gps eyeball during the south american total solar eclipse on 2nd july 2019," *Scientific Reports*, vol. 10, 2020.

[17] B. Emirant, K. Simon, and J. Edward, "Tracking the ionospheric response to the solar eclipse of November 3 2013," *International Journal of Atmospheric Sciences*, vol. 2014, Article ID 127859, 10 pages, 2014.

[18] Y. Heng, M. Enrique, and H.-P. Manuel, "Detection and description of the different ionospheric disturbances that appeared during the solar eclipse of 21st august 2017," *Remote Sensing*, vol. 10, 2018.

[19] S. Panda, S. Gedam, G. Rajaram, S. Sripathi, and A. Bhaskar, "Impact of 15 January 2010 annular solar eclipse on the equatorial and low latitude ionosphere over Indian region from Magnetometer, Ionosonde and GPS observations," 2018, https://arxiv.org/abs/1506.05245.

[20] H. M. Le, T. L. Tran, R. Fleury, T. T. Le, C. T. Nguyen, and H. T. Nguyen, "TEC variations and ionospheric disturbances during the magnetic storm in March 2015 observed from continuous GPS data in the Southeast Asia region," *Vietnam Journal of Earth Sciences*, vol. 38, no. 3, pp. 287–305, 2016.

[21] Z. Yang and Z. Liu, "Correlation between ROTI and ionospheric scintillation indices using Hong Kong low-latitude GPS data," *GPS Solutions*, vol. 20, no. 4, pp. 815–824, 2015.

[22] S. Datta-Barua, P. Doherty, S. Delay, T. Dehel, and J. Klobuchar, "Ionospheric scintillation effects on single and dual frequency GPS positioning," in *Proceedings of the 16th International Technical Meeting of the Satellite Division of The Institute of Navigation*, San Diego, CA, USA, 2003.

[23] K. M. Groves, S. Basu, J. M. Quinn et al., "A comparison of GPS performance in a scintillation environment at Ascension island,," in *Proceedings of the 13th International Technical Meeting of the Satellite Division of The Institute of Navigation (ION GPS 2000)*, pp. 672–679, Salt Lake City, UT, USA, 2000.

[24] L. Xifeng, Y. Yunbi, T. Bingfeng, and L. Min, "Observational analysis of variation characteristics of GPS-Based TEC fluctuations over China," *International Journal of Geo-information*, vol. 5, 2016.

[25] V. Annelie, "OpenUCT. retrieved from university of cape town," 2019, http://open.uct.ac.za/handle/11427/31337.

[26] Y. Norsuzila, M. F. Wan, F. Nor, L. Azita, and H. Mohamad, "GPS ionospheric scintillation and total electron content during partial solar eclipse in Malaysia," in *2014 IEEE 10th International Colloquium on Signal Processing & its Applications*, Kuala Lumpur, Malaysia, 2014.

[27] M. M. Alizadeh, H. Schuh, S. Zare, S. Sobhkhiz-Miandehi, and L. C. Tsai, "Remote sensing ionospheric variations due to total solar eclipse using GNSS observations," *Geodesy and Geodynamics*, vol. 11, no. 3, pp. 202–210, 2020.

[28] G. Seemala and C. Valladares, "Statistics of total electron content depletions observed over the south american continent for the year 2008," *Radio Science*, vol. 46, 2011.

[29] E. Sardo'n and N. Zarraoa, "Estimation of total electron content using GPS data: how stable are the differential satellite and reciever instrumental biases?" *Radio Science*, vol. 32, no. 5, pp. 1899–1910, 1997.

[30] C. M. Ngwira, J. Klenzing, J. Olwendo, F. M. D'ujanga, R. Stoneback, and P. Baki, "A study of intense ionospheric scintillation observed during a quiet day in the East African low latitude region," *Radio Science*, vol. 48, no. 4, pp. 396–405, 2013.

[31] P. Opio, F. D'ujanga, and T. Ssenyonga, "Latitudinal variation of the ionosphere in the African sector using GPS TEC data," *Advances in Space Research*, vol. 55, no. 6, pp. 1640–1650, 2015.

[32] J. B. Habarulema, Z. T. Katamzi, E. Yizengaw, Y. Yamazaki, and G. Seemala, "Simultaneous storm time equatorward and poleward large-scale TIDs on a global scale," *Geophysical Research Letters*, vol. 43, no. 13, pp. 6678–6686, 2016.

[33] S. Aryal, G. Geddes, S. Finn et al., "Multispectral and multinstrumentation observation of TIDs following the total solar eclipse of 21 August 2017," *Journal of Geophysical Research: Space Physics*, vol. 124, 2019.

[34] T. K. Zama and J. B. Habarulema, "Traveling ionospheric disturbances observed at South African midlalitudes during the 29-31 October 2003 geomagnetically disturbed period," *Advances in Space Research*, vol. 53, no. 1, pp. 48–62, 2013.

[35] T. Vincenty, "Direct and Inverse solutions of geodesics on the ellipsoid with applications of nested equations," *Survey Review*, vol. 23, no. 176, pp. 88–93, 1975.

[36] X. Pi, A. J. Mannucci, U. J. Lindqwister, and C. M. Ho, "Monitoring of global ionospheric irregularities using worldwide GPS network," *Geophysical Research Letters*, vol. 24, no. 18, pp. 2283–2286, 1997.

[37] R. Choudhary, J. St Maurice, K. Ambili, S. Surendra, and B. Pathan, "The impact of the January 15, 2010, annular solar eclipse on the equatorial and low latitude ionospheric densities," *Journal of Geophysical Research*, vol. 116, no. A9, 2011.

[38] G. Keith, M. William, C. Charles, and C. Ron, *GPS Positioning Errors in Solar Cycle 24*, Boston college, Chestnut Hill, MA, USA, 2012.

[39] P. Vadym, C. Charles, G. Keith et al., *GPS Observations of Plasma Bubbles and Scintillations over Equatorial Africa*, Boston college, Chestnut Hill, MA, USA, 2012, https://indico. ictp.it/event/a11159/session/77/contribution/50/material/0/ 0.pdf.